Nanostructured PtRu/C as Anode Catalysts Prepared in a Pseudomicroemulsion with Ionic Surfactant for Direct Methanol Fuel Cell

Weilin Xu, Tianhong Lu, Changpeng Liu, and Wei Xing*

State Key Laboratory of Electro-analytical Chemistry, Changchun Institute of Applied Chemistry, Graduate School of the Chinese Academy of Sciences, 5625 Renmin Street, Changchun 130022, Jilin, P. R. China

Received: March 20, 2005; In Final Form: May 7, 2005

Nanostructured PtRu/C catalysts have been prepared from a water-in-oil pseudomicroemulsion with the aqueous phase of a mixed concentrated solution of H_2PtCl_6, $RuCl_3$, and carbon powder, oil phase of cyclohexane, ionic surfactant of sodium dodecylbenzene sulfonate ($C_{18}H_{29}NaO_3S$), and cosurfactant *n*-butanol ($C_4H_{10}O$). Two different composing PtRu/C nanocatalysts (catalyst **1**, Pt 20 wt %, Ru 15 wt %; catalyst **2**, Pt 20 wt %, Ru 10 wt %) were synthesized. The catalysts were characterized by transmission electron microscopy, X-ray diffractometry, X-ray photoelectron spectroscopy, and thermogravimetric analysis, and the particles were found to be nanosized (2−4 nm) and inherit the Pt face-centered cubic structure with Pt and Ru mainly in the zero valance oxidation state. The ruthenium oxide and hydrous ruthenium oxide (RuO_xH_y) were also found in these catalysts. The cyclic voltammograms (CVs) and chronoamperometries for methanol oxidation on these catalysts showed that catalyst **1** with a higher Ru content (15 wt %) has a higher and more durable electrocatalytic activity to methanol oxidation than catalyst **2** with low Ru content (10 wt %). The CV results for catalysts **1** and **2** strongly support the bifunctional mechanism of PtRu/C catalysts for methanol oxidation. The data from direct methanol single cells using these two PtRu/C as anode catalysts show the cell with catalyst **1** has higher open circuit voltage (OCV = 0.75 V) and maximal power density (78 mW/cm^2) than that with catalyst **2** (OCV = 0.70 V, P_{max} = 56 mW/cm^2) at 80 °C.

Introduction

The direct methanol fuel cell (DMFC) has been considered as a suitable power source for portable applications avoiding any hydrogen storage problems.[1−3] However, there are several barriers to their application, including methanol crossover through the Nafion membrane[4] causing poisoning of the cathode, as well as substantial power losses due to the relatively low activity of the methanol electrooxidation catalysts currently in use. Improvements are needed in these areas before DMFCs can enter the market.[5]

Although many different electrocatalysts for methanol oxidation have been investigated, such as binary[6] or ternary compounds,[7,8] the benchmark anode catalyst for DMFC is still PtRu. First reported during the mid-1960s,[9−11] PtRu systems are the most studied and among the most active anode catalysts for the electrooxidation of MeOH.[12−15] It is well-known that the oxidation of methanol on platinum catalysts generates CO as an intermediate, which is a poison that adsorbs on the active sites of the catalyst. Ru forms an oxygenated species at lower potentials than Pt, and its presence in the catalyst promotes the oxidation of CO to CO_2 through the bifunctional mechanism.[16−17]

Several methods for the preparation of a Pt−Ru nanoparticle have been described,[18−39] such as the impregnation method,[29,30] colloidal method,[31−34] and microemulsion method.[35−41] As for the microemulsion method, since the 1940s, the term microemulsion was first defined by Schulman and Friend,[39a] and microemulsions have found a wide range of applications, including the preparation of PtRu nanoparticles as electrocatalysts for methanol oxidation.[38−40] Just as Chan[38b] or Sara[38c] reviewed, many kinds of metal nanoparticles, including PtRu bimetallic catalysts,[38,40] were synthesized from microemulsion by two ways: one is by mixing the two microemulsions, and the other is by directly adding the reducing agents to the microemulsions. Zhang et al.[39] synthesized PtRu unsupported nanoparticles with the nonionic surfactant Triton-100 as a surfactant. Liu[40a] reported the supported PtRu/C catalysts prepared with nonionic surfactants poly(oxyethylene)$_n$nonyl phenol ether (NP-n) and the reducing reagent HCHO. Escudero[40b] also explored highly dispersed PtRu/C catalysts for a H_2/O_2 fuel cell by microemulsion with a nonionic surfactant of alcohol ethoxylates (Berol 050). All the above PtRu catalysts were prepared based on nonionic surfactants; however, the ionic surfactants have rarely been used in microemulsion to prepare PtRu nanoparticles. Recently, Islam[41] studied the dispersancy of different surfactants to a carbon nanotube, such as ionic surfactants sodium dodecylbenzene sulfonate (NaDDBS, $C_{12}H_{25}C_6H_4SO_3Na$) and NaDBS ($C_4H_9C_6H_4SO_3Na$) and nonionic surfactants Triton-100 and DTAB. The results show that the dispersancy of NaDDBS to carbon is much higher than those of nonionic surfactants such as Triton-100 and DTAB or other ionic surfactants. In this work, we chose NaDDBS as the surfactant to prepare carbon-supported PtRu nanoparticles.

In the following, we report a simple method to prepare nanostructured PtRu/C catalysts by metastable water-in-oil pseudomicroemulsion of water solution/NaDDBS/*n*-butanol/cyclohexane/Cabot Vulcan XC-72 carbon powder. The nanostructured PtRu/C catalysts were characterized by transmission electron microscopy (TEM), X-ray diffractometry (XRD), X-ray photoelectron spectroscopy (XPS), thermogravimetric analysis (TGA), and electrochemical methods, such as cyclic voltam-

* To whom correspondence should be addressed. E-mail: xingwei@ciac.jl.cn. Tel: 86-431-5262225. Fax: 86-431-5685653.

10.1021/jp051443y CCC: $30.25
Published on Web 07/07/2005

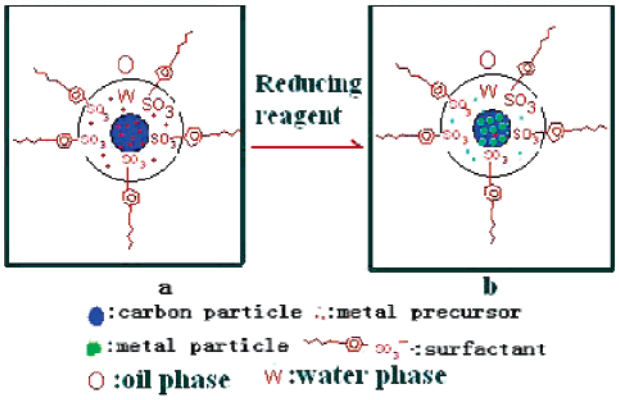

Figure 1. Preparation mechanism of PtRu/C in pseudomicroemulsion: (a) the metal precursor adsorbed on carbon, (b) the metal particle aggraded on carbon.

metry (CV) and chronoamperometry (CA). The performance of a single cell of DMFC with these anode electrocatalysts was also evaluated.

Experimental Section

Ionic surfactant sodium dodecylbenzene sulfonate ($C_{18}H_{29}NaO_3S$, NaDDBS) with high dispersibility from Sigma Chemical Co. was used as received. Cosurfactant *n*-butanol ($C_4H_{10}O$) and oil phase cyclohexane (C_6H_{12}) were from J&K China Chemical Ltd. The metal sources were an aqueous solution of H_2PtCl_6 and $RuCl_3$ freshly prepared in order to avoid the formation of complex $[RuO(H_2O)_4]^{2+}$ present in aged solutions, which is difficult to be reduced.[44] Deionized water (18.2 MΩ) was produced by a Milli-Q ultrapure system from Millipore Ltd., USA. The preparation of Pt−Ru /C electrocatalysts was the following or as shown in Figure 1. The Vulcan XC-72 carbon black, which was previously treated by poly(vinyl alcohol) (Sigma Chemical Co. $M_n = 2000$) to improve its hydrophilicity, was added to the mixed concentrated solution of H_2PtCl_6 and $RuCl_3$ with stirring for 12 h. Then continuous oil-phase cyclohexane, the surfactant, and cosurfactant were added in that order with stirring, and the volume fraction of the oil phase is 2-fold of the dispersed aqueous phase. The resulting slurry is a gray metastable water-in-oil pseudomicroemulsion due to the existence of carbon powder. The water phase of the pseudomicroemulsion is dispersed in the continuous oil phase, which is immiscible to the metal precursors contained in water. The pseudomicroemulsion has a core of carbon nanoparticles, which absorbs many precursors, such as $PtCl_6^{2-}$ or Ru^{3+}, as shown in Figure 1a. The size of the core is in the order of tens of nanometers to hundreds of nanometers. The pH value of the slurry was adjusted to 9 by adding a concentrated solution of Na_2CO_3. The reducing reagent of $NaBH_4$ solution (for catalyst **1**) or HCHO solution (for catalyst **2**) was dropped into the slurry with stirring to reduce the metal precursors, and then the nucleation and growth of metal particles take place on the surface of the active carbon shown in Figure 1b. The mixture was separated centrifugally, then washed repeatedly with water at 80 °C to remove the residual PVA and last washed three times with ethanol to remove the organics. The resulting catalysts were air-dried at 80 °C in a drying oven for 24 h and then kept in desiccator.

The Pt−Ru/C catalysts were characterized by a JEOL 2010FX transmission electron microscope. For microscopic examinations, the samples were first ultrasonicated in alcohol for 1 h and then deposited on 3 mm Cu grids. The samples were also analyzed by XPS on a (VG ESCALAB MK II) X-ray spectrometer. XPS spectra were recorded by a Phi Quantum 2000 XPS system (Physical Electronics, Inc.) using Al Kα radiation at a base pressure below 5×10^{-9} Torr. Narrow scan photoelectron spectra were recorded for Pt 4f, C 1s, and Ru 3d. Peak deconvolution was performed using the curve-fitting program VGX900. XRD measurements were performed on a (Rigaku D/max 2500 VPC) X-ray diffractormeter using Cu Kα radiation ($\lambda = 0.1542$ nm). TGA was performed on a Perkin-Elmer computer/thermal analyzer to obtain thermograms with a scan rate of 10 °C/min under N_2 at a flow rate of 75 mL/min.

An EG&G model 273 potentiostat/galvanostat and a conventional three-electrode test cell were used for electrochemical measurements. The working electrode was a thin layer of Nafion impregnated catalyst cast on a glassy carbon disk held in a Teflon cylinder. The catalyst layer was obtained in the following way: (i) a slurry was first prepared by sonicating for 1 h a mixture of 1 mL of alcohol, 5 mg of PtRu/C catalyst, and 50 μL of Nafion solution (Aldrich, 5 w/o Nafion); (ii) 6 μL of the slurry was pipetted and spread on the glassy carbon disk; (iii) the electrode was then dried at 80 °C for 1 h. The surface area of the glassy carbon disk was 0.196 cm^2. A Pt foil electrode and a Ag/AgCl were used as the counter and reference electrodes, respectively. All potentials in this report are quoted against Ag/AgCl. All electrolyte solutions were deaerated by high-purity argon for 15 min prior to any measurement. The electrolyte solution was 0.5 M CH_3OH in 0.5 M H_2SO_4, which was prepared from high-purity sulfuric acid, high-purity grade methanol, and distilled water. For cyclic voltammetries of methanol oxidation, the electrode was activated by cycling the potential between −0.2 and 1.1 V vs Ag/AgCl at 10 mV/s. For chronoamperometry, the electrode potential was fixed at 0.5 V vs Ag/AgCl.

The MEAs (membrane electrode assemblies) for the DMFC test cell were made by hot-pressing ($T = 120$ °C, $P = 4$ MPa) pretreated Nafion 117 together with an anode sheet and a cathode sheet. The anode sheet was a carbon paper (SGL, Germany) with a carbon-supported PtRu catalyst layer. The cathode sheet was a carbon paper with a carbon-supported 20 wt % Pt catalyst layer supplied by E-TEK. The Pt loadings at the anode and cathode were 1.5 and 2 mg/cm^2, respectively, and the effective electrode area was 4 cm^2. The fuel was 2 M CH_3OH delivered at 2 mL/min by a micropump, and the oxygen pressure was 1.6 atm. The working temperature is 80 °C. To characterize the performance stability of different MEAs, three MEAs were tested for catalysts **1** and **2**, respectively, under the same conditions.

Results and Discussion

Physicochemical Characterization of PtRu/Vulcan Carbon Electrocatalysts. In our work, two kinds of PtRu bimetallic nanoparticles with different Ru content are prepared by reducing reagents of $NaBH_4$ (catalyst **1:** Pt 20 wt %, Ru 15 wt %) and HCHO solution (catalyst **2:** Pt 20 wt %, Ru 10 wt %), respectively. The size of the alloy particles was analyzed by TEM measurement. Parts a and b of Figure 2 show typical TEM images for catalysts **1** and **2**, showing a remarkably uniform and high dispersion of metal particles on the active carbon surface. The size distributions of the metal particles on the carbon were obtained by measuring the sizes of 150 randomly chosen particles in the magnified TEM images (e.g., Figure 2c for the PtRu particles reduced by $NaBH_4$). The average diameters of 3.2 ± 0.3 nm for PtRu particles reduced by $NaBH_4$ and 3.4 ± 0.3 nm for particles reduced by formaldehyde were accompanied by relatively narrow particle size distributions

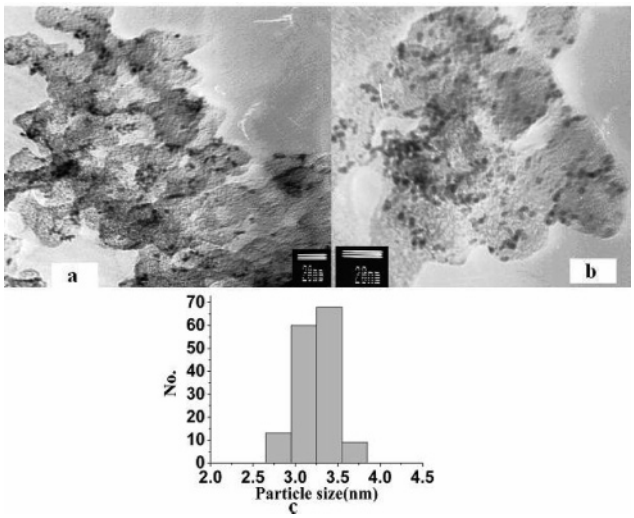

Figure 2. TEM images of pseudoemulsion-synthesized PtRu/Vulcan Carbon electrocatalysts: (a) catalyst **1** with reducing agent of $NaBH_4$, (b) catalyst **2** with reducing agent of formaldehyde. (c) Particle size distribution for the PtRu nanoparticles with reducing agent of $NaBH_4$.

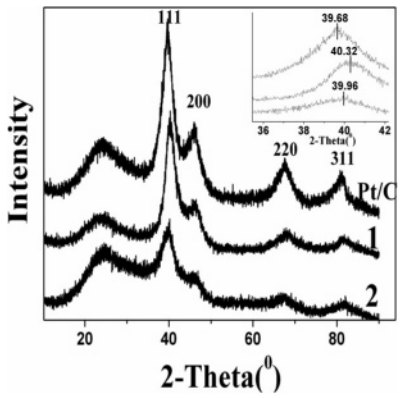

Figure 3. XRD patterns of Pt/C and PtRu catalysts: **1**, catalyst **1**; **2**, catalyst **2**.

(2−4 nm). The size of catalyst **2** is larger than that of catalyst **1**. This result is consistent with the previous result.[40a] The size of PtRu particles prepared by Liu[40a] with a reducing reagent of HCHO and surfactant of NP-n is somewhat larger (>4.3 nm) and widely dispersed (4−20 nm). The relatively larger size and wide dispersion of particles probably can be attributed to the relatively lower reductivity of HCHO compared with $NaBH_4$ and the lower dispersibility of NP-n compared with NaDDBS, which can provide a uniform environment for the nucleation and growth of metal particles.

The XRD patterns for PtRu/Vulcan carbon catalysts are shown in Figure 3 alongside the diffraction pattern of a Vulcan-carbon-supported Pt catalyst used as a comparison. All PtRu catalysts displayed the characteristic patterns of Pt faced-centered cubic (fcc) diffraction, except that the 2θ values were all shifted slightly to higher values (shown in the inset, a partial magnification). The shift in 2θ in PtRu curves corresponds to a decrease in the lattice constant due to the incorporation of Ru atoms.[38−42] The diffraction peaks in PtRu catalysts match the (111), (200), (220), and (311) characteristics of a platinum fcc structure. There were no observable lines in the XRD spectra corresponding to those of pure Ru or RuO_2. It should be noted that the shift in 2θ for catalyst **2** is smaller than that of **1**; the reason probably is the lower Ru content and less Ru atoms incorporate into Pt crystal lattice in catalyst **2**. As for low content amorphous and defective RuO_xH_y speciation, the XRD cannot

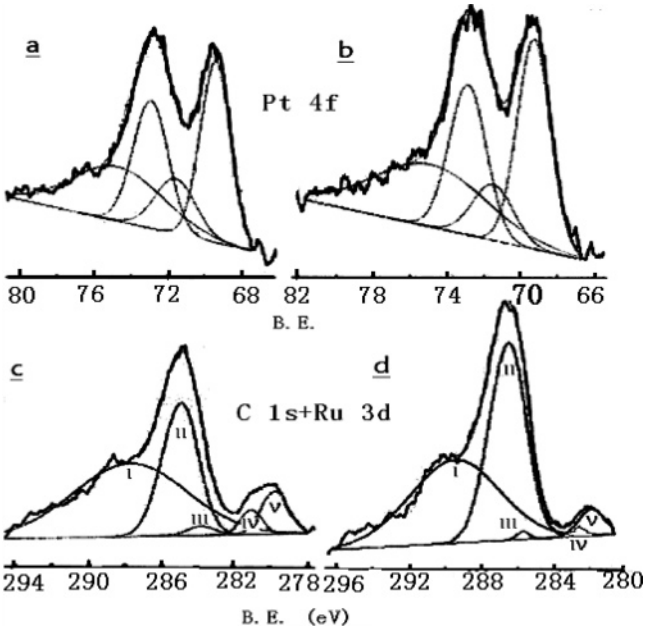

Figure 4. X-ray photoelectron spectra of the PtRu/C catalysts (**1** and **2**). (a) and (c) are the Pt 4f spectra and C 1s and Ru 3d spectra for catalyst **1**, respectively; (b) and (d) are those for catalyst **2**.

TABLE 1: Content of Different Speciations in Catalysts

relative content	Ru (0)	RuO_2	RuO_xH_y	Pt(0)	Pt(II)
catalyst **1**	0.60	0.26	0.14	0.60	0.40
catalyst **2**	0.79	0.11	0.1	0.57	0.43

reflect their existence.[44] So these XRD spectra can only indicate that a homogeneous solid solution of PtRu was mainly formed at the atomic level with a basically unaltered fcc structure and probably there are some RuO_xH_y at the nanoparticle surface. The existence of RuO_xH_y will be confirmed by the following XPS and TGA results. The average alloy particle sizes were calculated by the Scherrer equation from the peaks that match the (220) characteristic.[44] The calculation results, which estimated the average size of 3.1 nm for the PtRu particles reduced by $NaBH_4$ and 3.3 nm for the PtRu reduced by formaldehyde, are in good agreement with the TEM measurements.

XPS was used to determine the surface oxidation states of the catalytic and cocatalytic metals. As most of the atoms are on the surface, the oxidation state measured as such would reflect the bulk oxidation state. Figure 4 shows the Pt 4f, C 1s, and Ru 3d regions of the XPS spectrum of PtRu/C catalysts of **1** and **2**. The Ru 3p signals for them are too weak to be analyzed. The Pt spectra (parts a and b of Figure 4) can be fitted by two pairs of overlapping Lorentzian curves. The most intense peaks (70.1 and 73.4 eV) were due to metallic Pt. The second set of doublets (71.6 and 74.8 eV), observed at BE 1.4 eV higher than Pt(0), could be attributed to the Pt(II) chemical state on PtO or $Pt(OH)_2$.[46] The relative areas indicate that metallic Pt^0 is the predominant species shown in Table 1. The entire Ru 3d + C 1s envelopes were deconvolved for the two catalysts. The envelopes are fitted with two C 1s peaks and three Ru $3d_{5/2}$ peaks shown in parts c and d of Figure 4 for the **1** and **2**, respectively. The C 1s spectrum (peaks I and II) appeared to be composed of graphitic carbon (284.6 eV) and a −C═O like species (287.7 eV). The Ru $3d_{5/2}$ signal was deconvoluted into three distinguishable pairs of peaks of different intensities at BE = 279.7, 281.1, and 283.8 eV, corresponding to Ru(0) (peak V), RuO_2 (peak IV), and hydrous ruthenium oxide (RuO_xH_y, peak III), respectively. These hydrous ruthenium oxides are

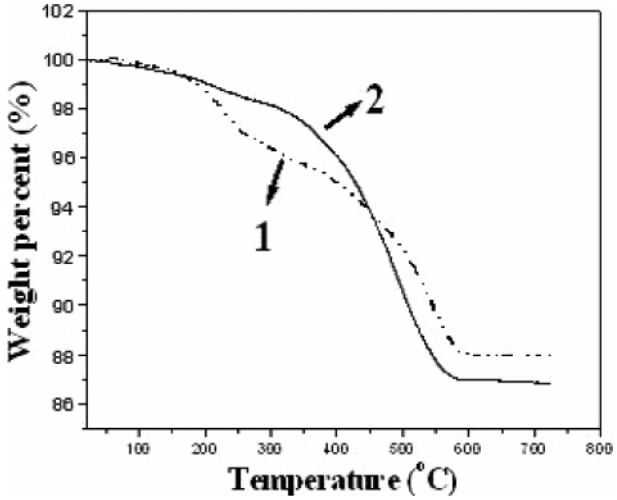

Figure 5. TGA scans in following N_2 for PtRu/C catalysts (**1**, catalyst **1**; **2**, catalyst **2**). Temperature was ramped at 10 °C/min.

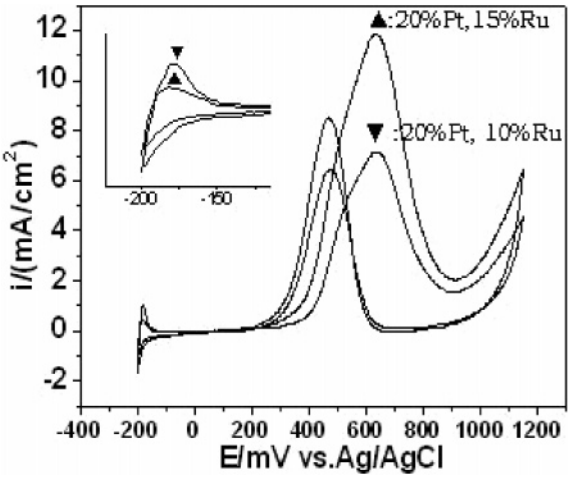

Figure 6. Cyclic voltammograms of different PtRu/C catalysts/glassy carbon electrode in 0.5 M methanol + 0.5 M H_2SO_4 solution at room temperature at a scan rate of 10 mV/s. Pt loading at 0.03 mg/cm^2.

reasonable electron and proton conductors.[45] Recently it was found[45] that these species are of key importance in the mechanism proposed for direct methanol oxidation; in particular, Ru−OH is a critical component of the bifunctional mechanism proposed for direct methanol oxidation.[44,45] The relative content of different ruthenium speciation in these two different electrocatalysts is also shown in Table 1. It clearly shows that Ru(0) is the predominant species and catalyst **1** contains more RuO_xH_y than catalyst **2**, while catalyst **2** contains more PtO_xH_y (Pt(II)) than catalyst **1**.

TGA was performed on the PtRu/C catalysts (**1** and **2**). The TGA curves obtained under following N_2 with scan rate of 10 °C/min are shown in Figure 5. The weight losses are 4% and 2% for catalysts **1** and **2** under 300 °C, respectively. The water (including physisorbed water and structure water) of the hydrous ruthenium oxide is lost mainly under 300 °C. according to Rolison's result.[44] So this low-temperature weight loss from catalysts is presumably due to the water loss from hydrous Ru or Pt oxide phases detected by the above XPS experiments or reported by others.[45,47] After 400 °C, the weight loss of catalyst **2** is faster than that of **1**. Upon 600 °C, the weight loss of catalyst **2** is 13%, while that for catalyst **1** is 12%. Catalyst **2** has a higher content (43%) of Pt(II) than catalyst **1** (40%), according to the above result of XPS for Pt 4f shown in Table 1. So the high-temperature loss probably can be attributed to hydrous platinum oxide. The above results probably also indicate that catalyst **1** contains more RuO_xH_y, while catalyst **2** contains more PtO_xH_y.

Electrochemical Performances. The PtRu/C electrocatalysts (**1** and **2**) prepared by the pseudomicroemulsion method were characterized at room temperature by cyclic voltammetry (CV) in electrolytes of 0.5 M H_2SO_4 and 0.5 M CH_3OH at a scan rate of 10 mV/s with Pt loading of 0.03 mg/cm^2 shown in Figure 6. The onset of methanol oxidation peaks for **1** was observed at 0.25 V vs Ag/AgCl while that for **2** was observed at 0.3 V vs Ag/AgCl. The large methanol oxidation peak was around 0.62 V vs Ag/AgCl for these two electrocatalysts, and **1** had a nearly 2-fold peak current to that of **2**. At the peak, the current densities are 400 mA/mg of Pt and 200 mA/mg of Pt for catalysts **1** and **2**, respectively, with a scan rate of 10 mV/s. The current density for the PtRu particles with a size of 2.5 nm prepared by Zhang et al.[39] is only 250 mA/mg of Pt with a higher scan rate of 25 mV/s and 1.0 M CH_3OH. Liu's PtRu/C catalysts[40] with larger sizes (>4.3 nm) prepared with the surfactant of NP-n had much lower current densities. This probably indicates that 3−4 nm is the optimal size for PtRu nanoparticles to catalyze methanol oxidation. The peak potentials for catalysts **1** and **2** are lower compared with that on the pure Pt electrode. The peaks on the reverse scan near 0.45 V vs Ag/AgCl were due to the reactivation of the oxidized Pt oxide and the oxidation of methanol and the intermediates.

The inset (Figure 6) is the partial magnification in the range of hydrogen adsorption/desorption. The peak area reflects the number of Pt active sites to hydrogen adsorption/desorption. It shows that **2** had much more Pt active sites to hydrogen adsorption/desorption than that of **1**. This is different from the above methanol oxidation peak currents. This difference indicates that there are latent active platinum atoms on catalysts **1** and **2**. The latent active platinum atoms are not active to hydrogen adsorption/desorption individually but can be active to methanol oxidation with the cooperation of RuO_xH_y. The higher content of RuO_xH_y in catalyst **1** shown in the XPS results promotes more latent active platinum atoms to be active for methanol oxidation or depoisons the Pt atoms from CO_{ad}. This phenomenon strongly supports the bifunctional mechanism, in which the Ru or RuO_xH_y can promote the oxidation of CO to CO_2.[16,17] In some articles,[48−54] the electrochemical surface areas for catalysts were obtained by a slow potential sweep, and the total number of Pt atoms on the electrode surface was determined by integrating the change in the region of hydrogen adsorption/desorption in the cyclic voltammograms. Our results here, however, clearly indicate that there are many special active Pt atoms on Pt nanoparticles, which are not active to hydrogen adsorption/desorption but can be active to methanol oxidation with the cooperation of RuO_xH_y, and so the above method to determine the number of active atoms is only reasonable for Pt monometal catalysts but not reasonable for Pt-based catalysts which contain some kind of promoters, such as Ru.

Figure 7 shows plots of current vs time for the electrooxidation of MeOH at 22 °C (E = 0.5 V vs Ag/AgCl) on different PtRu/C catalysts with the chronoamperometry (CA) method. These curves reflect the activity and stability of different catalysts to catalyze methanol oxidation. Obviously, the decay in the methanol oxidation current with time was different. Catalyst **1** has higher initial current and limiting current than those of **2**, which indicate a better catalytic activity and stability to methanol oxidation of **1** than to that of **2**. This result is consistent with that of CVs.

The pseudomicroemulsion-prepared PtRu/C catalysts were used as anode catalysts in a single DMFC test cell. The catalyst

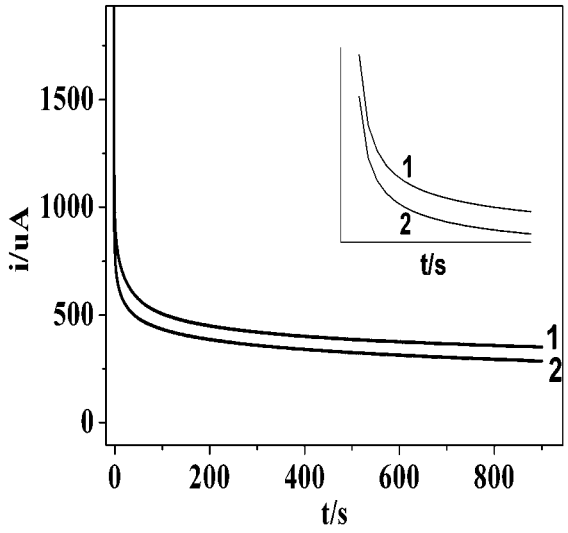

Figure 7. Current vs time plots of chronoamperometry for the electrooxidation of methanol in 0.5 M CH_3OH/0.5 M H_2SO_4 electrolytes at 0.5 V vs Ag/AgCl at room temperature. The inset is the magnification of the initial currents. **1**, catalyst **1**; **2**, catalyst **2**.

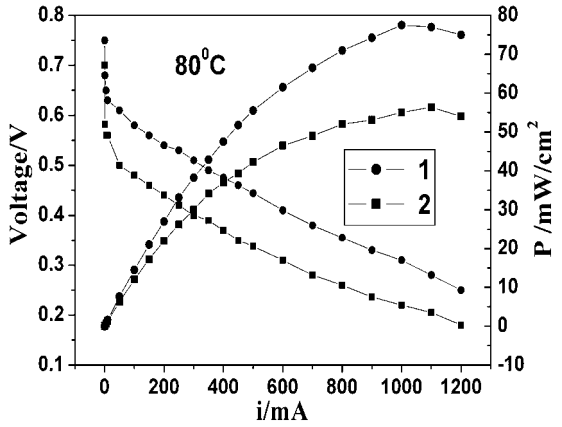

Figure 8. *I*−*V* characteristics and output power of a single cell at operating temperature of 80 °C: anode, PtRu/Vulcan carbon (1.5 mg Pt/cm^2), 2 M CH_3OH, 2 mL/min; cathode, Pt/C (E-TEK) (2 mg Pt/cm^2), pO_2 1.6 atm. **1**, catalyst **1**; **2**, catalyst **2**.

loadings at the anode and cathode were 1.5 mg of Pt/cm^2 PtRu/C and 2 mg of Pt/cm^2 Pt/C (20%), respectively. Steady-state polarization curves and the special power density curves at the operating temperature of 80 °C are obtained with three MEAs for catalysts **1** and **2**, respectively. The averaged results are shown in Figure 8. It is shown that the cells with catalyst **1** have higher averaged open circuit voltage (OCV = 0.75 V) and maximal power density (78 mW/cm^2) than those of catalyst **2** (OCV = 0.70 V, P_{max} = 56 mW/cm^2). This result is consistent with the above CV and CA results.

Conclusions

Nanostructured PtRu alloy particles supported on carbon were prepared from pseudomicroemulsion of a water solution/dodecylbenzene sulfonic acid sodium salt/*n*-butanol/cyclohexane/Cabot Vulcan XC-72 with two different reducing reagents $NaBH_4$ and HCHO, respectively. The TEM showed that the size of the particles is between 2 and 4 nm, and the strong reducing reagent can lead to smaller-sized nanoprarticles. XRD showed that these alloy particles show the characteristic structure of Pt fcc. XPS and TGA results indicate that the catalysts contained mainly Pt(0) and Ru(0) with some Pt(II) and RuO_xH_y. The CV results of these catalysts strongly support that the bifunctional mechanism and the activity of catalysts **1** or **2** are much higher than that of PtRu nanoparticles prepared with nonionic surfactants. CV, CA, and DMFC experiments show that the PtRu/C catalyst **1** with higher Ru content (15 wt %) has higher activity and stability toward methanol oxidation than catalyst **2** (10 wt %) with low Ru content.

Acknowledgment. The authors are grateful for the financial sponsors of State Key Fundamental Research Program of China (973 Program, G2000026408), State Key High Technology Research Program of China (863Program, 2001AA323060, 2003AA517062), and Nature Science Foundation of China (20373068, 20433060).

References and Notes

(1) Wasmus, S.; Küver, A. *J. Electroanal. Chem.* **1999**, *461*, 14.
(2) Carrette, L.; Collins, J.; Dickinson, A.; Stimming, U. *Bunsen Mag.* **2000**, *2*, 27.
(3) Hamnett, A.; Troughton, G. *Chem. Ind.* **1992**, *7*, 480.
(4) Ramya, K.; Dhathathreyan, K. S. *J. Electroanal. Chem.* **2003**, *542*, 109.
(5) Wasmus, S.; Küver, A. *J. Electroanal. Chem.* **1999**, *461*, 14.
(6) Grgur, B.; Markovic, N.; Ross, P. N. *Electrochim. Acta* **1998**, *43* (24), 3631.
(7) Gotz, M.; Wendt, H. *Electrochim. Acta* **1998**, *43* (24), 3637.
(8) Bett, J.; Kunz, H.; Aldykiewicz, A., Jr.; Fenton, J.; Bailey, W.; McGrath, D. *Electrochim. Acta* **1998**, *43* (24), 3645.
(9) Frumkin, A. N.; Podlovchenko, B. I. *Ber. Akad. Wiss. U.S.S.R.* **1963**, *150*, 34.
(10) Bockris, J. O.′M.; Wroblowa, H. *J. Electroanal. Chem.* **1964**, *7*, 428.
(11) Petry, O. A.; Podlovchenko, B. I.; Frumkin, A. N.; Lal, H. *J. Electroanal. Chem.* **1965**, *10*, 253.
(12) Ren, X. M.; Zelenay, P.; Thomas, S.; Davey, J.; Gottesfeld, S. *J. Power Sources* **2000**, *86*, 111.
(13) McNicol, B. D.; Rand, D. A. J.; Williams, K. R. *J. Power Sources* **1999**, *83*, 15.
(14) Wasmus, S.; Kuver, A. *J. Electroanal. Chem.* **1999**, *461*, 14.
(15) Kordesch, K.; Simader, G. *Fuel Cells and their Applications*; VCH: Weinheim, Germany, 1996.
(16) Gasteiger, H. A.; Markovic, N. M.; Ross, P. N., Jr. *J. Phys. Chem.* **1995**, *99*, 8290.
(17) Watanabe, M.; Motoo, S. *J. Electroanal. Chem.* **1975**, *60*, 267.
(18) Roth, C.; Martz, N.; Fuess, H. *Phys. Chem. Chem. Phys.* **2001**, *3*, 315.
(19) Taylor, E.; Anderson, E.; Vilambi, N. *J. Electrochem. Soc.* **1992**, *139*, L45.
(20) Verbrugge, M. W. *J. Electrochem. Soc.* **1994**, *141*, 46.
(21) Watanabe, M.; Uchida, M.; Motoo, S. *J. Electroanal. Chem.* **1987**, *229*, 395.
(22) Radmilovic, V.; Gasteiger, H. A.; Ross, P. N., Jr. *J. Catal.* **1995**, *154*, 98.
(23) Alerasool, S.; Gonzalez, R. D. *J. Catal.* **1990**, *124*, 204.
(24) Bonnemann, H.; Brinkmann, R.; Brijoux, W.; Dinjus, E.; Joussen, T.; Korall, B. *Angew. Chem. Int., Ed. Engl.* **1991**, *30*, 804.
(25) Gonzalez, E. R.; Ticianelli, E. A.; Pinheiro, A. L. N. J. Perez, Brazilian Patent. INPI-SP No. 00321, 1997.
(26) Goodenough, J. B.; Hamnett, A.; Kennedy, B. J.; Manoharan, R.; Weeks, S. A. *Electrochim. Acta* **1990**, *35*, 199.
(27) Brus, L. *J. Phys. Chem.* **1986**, *90*, 2555.
(28) Joo, S. H.; Choi, S. J.; Oh, I.; Kwak, J.; Liu, Z.; Terassaki, O.; Ryoo, R. *Nature* **2001**, *412*, 169.
(29) Zoval, J. V.; Lee, J.; Gorer, S.; Penner, R. M. *J. Phys. Chem. B* **1998**, *102* (7), 1166.
(30) Joo, S. H.; Choi, S. J.; Oh, I.; Kwak, J.; Liu, Z.; Terassaki, O.; Ryoo, R. *Nature* **2001**, *412*, 169.
(31) Curtis, A.; Duff, D.; Edwards, P.; Jefferso, D.; Johnson, B.; Kirkland A.; Wallace, A. *J. Phys. Chem.* **1988**, *92*, 2270.
(32) Cardenas-Trivino, G.; Klabunde, K.; Brock, D. E. *Langmuir* **1987**, *3*, 986.
(33) Franke, R.; Rothe, J.; Pollmann, J.; Hormes, J.; Bonnemann, H.; Brijoux, W.; Hindernburg, T. *J. Am. Chem. Soc.* **1996**, *118*, 12090.
(34) Vidoni, O.; Philippot, K.; Amiens, C.; Chaudret, B.; Balmes, O.; Malm, J. O.; Bovin, J. O.; Senocq, F.; Casanove, M. J. *Angew. Chem., Int. Ed.* **1999**, *38*, 3736.
(35) Wang, J.; Lee See Ee, S. C. Ng, Chew, C. H.; Gan, L. M. *Mater. Lett.* **1997**, *30*, 119.
(36) Lee, M. H.; Tai, C. Y.; Lu, C. H. *J. Eur. Ceram. Soc.* **1999**, *19*, 2593.

(37) Bommarius, A. S.; Holzarth, J. F.; Wang, D. I. C.; Hatton, T. A. *J. Phys. Chem.* **1990**, *94*, 7232.

(38) (a) Zhang, X.; Chan, K. Y. *J. Mater. Chem.* **2002**, *12*, 1203. (b) Chan, K. Y.; Ding, J.; Ren, J.; Cheng, S.; Tsang, K. Y. *J. Mater. Chem.* **2004**, *14*, 505−516; (c) Eriksson, S.; Nylén, U.; Rojas, S.; Boutonner, M. *Appl. Catal., A* **2004**, *265*, 207−219.

(39) (a) Schulman, J. H.; Friend, J. A. *J. Colloid Interface Sci*. **1949**, *4*, 497. (b) Zhang, X.; Chan, K. Y. *Chem. Mater*. **2003**, *15*, 451.

(40) (a) Liu, Z.; Lee, J.; Han, M.; Chen, W.; Gan, L. *J. Mater. Chem*. **2002**, *12*, 2453. (b) Escudero, M. J.; Hontanon, E.; Schwartzb, S.; Boutonnetb, M.; Dazaa, L. *J. Power Sources* **2002**, *106*, 206.

(41) Islam, M. F.; Rojas, E.; Bergey, D. M.; Yodh, A. G. *Nano Lett.* **2003**, *3*, 269−273.

(42) Chu, D.; ilman, S. *J. Electrochem. Soc.* **1996**, *143*, 1685.

(43) Iwasita, T.; Hoster, H.; John-Anacker, A.; Lin, W. F.; Vielstich, W. *Langmuir* **2000**, *16*, 522.

(44) Rolison, D. R.; Hagans, P. L.; Swider, K. E.; Long, J. W. *Langmuir* **1999**, *15*, 774.

(45) Warren, B. E. In *X-ray Diffraction*; Addison- Wesley: Reading, MA, 1996.

(46) Soryna, S. C. *Handbook of Stable Strontium*; Plenum Press: New York, 1981; p 11.

(47) Hagans, P. L.; Swider, K. E.; Rolison, D. R. In *Electrode materials and Processed for Energy Conversion and Storge IV*; McBreen J., Srinivasan S., Eds.; PV 97−13; Electrochemical Society: Pennington, NJ, 1997; pp 86−105.

(48) Perez, J.; Gonzalez, E. R.; Ticianelli, E. A. *Electrochim. Acta* **1998**, *44*, 1329.

(49) Tamizhmani, G.; Dodelet, J. P.; Guay, D. *J. Electrochem. Soc.* **1996**, *143*, 18.

(50) Fournier, J.; Faubert, G.; Tilquin, J. Y.; Cote, O. R.; Guay, D.; Dodelet, J. P. *J. Electrochem. Soc.* **1997**, *144*, 146.

(51) Gloaguen, F.; Andolfatto, F.; Durand, R.; Ozil, P. *J. Appl. Electrochem.* **1994**, *24*, 861.

(52) Ciureanu, M.; Wang, H. *J. Electrochem. Soc*. **1999**, *146*, 4031.

(53) Ticianelli, E. A.; Beery, J. G.; Srinivasan, S. *J. Appl. Electrochem*. **1991**, *21*, 597.

(54) Pozio, A.; De Francesco, M.; Cemmi, A.; Cardellini, F.; Giorgi, L. *J. Power Sources* **2002**, *105*, 13.